

# Mapping Disaster Areas Jointly: RFID-Coordinated SLAM by Humans and Robots

Alexander Kleiner, C. Dornhege and D. Sun

## Post Print

N.B.: When citing this work, cite the original article.

©2007 IEEE. Personal use of this material is permitted. However, permission to reprint/republish this material for advertising or promotional purposes or for creating new collective works for resale or redistribution to servers or lists, or to reuse any copyrighted component of this work in other works must be obtained from the IEEE.

Alexander Kleiner, C. Dornhege and D. Sun, Mapping Disaster Areas Jointly: RFID-Coordinated SLAM by Humans and Robots, 2007, *IEEE Int. Workshop on Safety, Security and Rescue Robotics (SSRR)*, 1-6.

<http://dx.doi.org/10.1109/SSRR.2007.4381263>

Postprint available at: Linköping University Electronic Press

<http://urn.kb.se/resolve?urn=urn:nbn:se:liu:diva-72542>

# Mapping disaster areas jointly: RFID-Coordinated SLAM by Humans and Robots

Alexander Kleiner, Christian Dornhege and Sun Dali  
*Institut für Informatik*  
*University of Freiburg*  
*79110 Freiburg, Germany*  
{kleiner,dornhege,sun}@informatik.uni-freiburg.de

**Abstract** — We consider the problem of jointly performing SLAM by humans and robots in Urban Search And Rescue (USAR) scenarios. In this context, SLAM is a challenging task. First, places are hardly re-observable by vision techniques since visibility might be affected by smoke and fire. Second, loop-closure is cumbersome due to the fact that firefighters will intentionally try to avoid performing loops when facing the reality of emergency response, e.g. while they are searching for victims. Furthermore, there might be places that are only accessible to robots, making it necessary to integrate humans and robots into one team for mapping the area after a disaster.

In this paper, we introduce a method for jointly correcting individual trajectories of humans and robots by utilizing RFID technology for data association. Hereby the poses of humans and robots are tracked by PDR (Pedestrian Dead Reckoning) and slippage sensitive odometry, respectively.

We conducted extensive experiments with a team of humans and robots within a semi-outdoor environment. Results from these experiments show that the introduced method allows to improve single trajectories based on the joint graph, even if they do not contain any loop.

**Keywords:** *SLAM, USAR, PDR, RFID*

## I. INTRODUCTION

Pedestrian navigation and localization is a growing field motivated from the context of Location Based Services (LBS) [15], navigation for the Blind [13], and emergency responder tracking [18]. Particularly in the field of emergency response, the efficiency of rescue teams, e.g. when performing the search for victims after a disaster, depends on their ability to coordinate and thus to be informed about their locations. Given the locations of rescue teams during emergency response, one could efficiently assign unexplored regions, either in a centralized [10] or decentralized way. However, to be aware of locations during exploration within collapsed buildings is a challenging task. In urban environments GNSS (Global Navigation Satellite System) positioning is affected by the *multipath propagation* problem [7]. Buildings in the vicinity of the receiver reflect GNSS signals, resulting in secondary path propagations with longer propagation time, causing erroneous position estimates. Furthermore, the ability to re-observe landmarks might be affected by limited visibility due to smoke and fire.

One solution to this problem is to equip firefighters with assistance systems, such as wearable devices [10], [18], per-

forming Simultaneous Localization And Mapping (SLAM) without cognitive load, e.g. without requiring interactions by the user. SLAM methods work with the principle of map improvement through loop-closure, i.e. to improve the map globally each time places have been re-observed. However, when facing the reality of emergency response, firefighters will intentionally try to avoid performing loops, e.g. while they are searching for victims. Furthermore, there might be places that are only accessible by robots, making it necessary to integrate humans and robots into one team for mapping the area after a disaster. In this

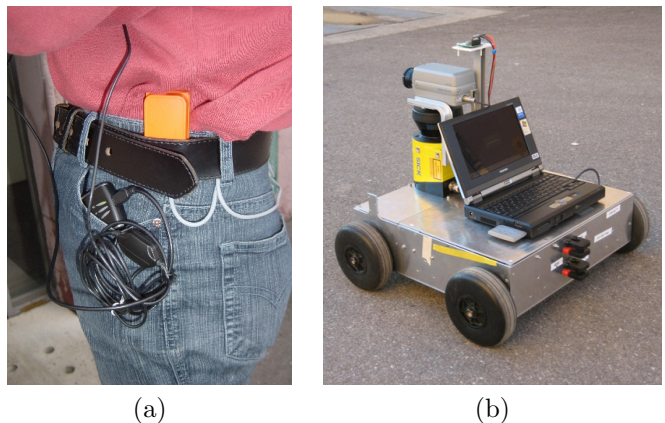


Fig. 1. Experimental setup: (a) The test person (the third author) with *Xsens MTi* IMU for walking detection. (b) the *Zerg* robot with over-constrained wheel odometry and *Xsens MTx* for pose tracking. Furthermore, a *Holux* GPS device has been utilized for obtaining ground truth data.

paper, we introduce a solution to this problem based on information sharing between pedestrians and robots by RFID technology. Hereby the pose of each pedestrian is automatically tracked by a PDR (Pedestrian Dead Reckoning) method, which recognizes human footsteps analytically from acceleration patterns. Robot poses are tracked from wheel odometry and IMU data only. For this purpose, we developed a slippage-sensitive odometry that reduces odometry errors on slippery ground, as for example, if the robot navigates on grass. Humans and Robots estimate the distances between RFID tags by pose tracking and communicate them to a central station. The central station successively builds a joint graph from these estimates and

corrects the joint network of all trajectories by minimizing the Mahalanobis distance [16], while utilizing RFID transponders for data association [11]. RFID technology offers many advantages within harsh environments: First, they can be operational up to temperatures of 450 °C [5]. Second, their size can be below a half millimeter, e.g. the  $\mu$ -Chip from *Hitachi*, making it possible to deploy them in masses within disaster areas, for example distributed by UAVs or UGVs [12].

Borenstein et al. introduced a method for improving the odometry on differential-drive robots [2]. A method for odometry improvement and optimization of motor control algorithms on 4WD robots has been introduced by Ojeda et al [19]. They applied “Expert Rules” in order to infer the occurrence of wheel slip. PDR methods have been extensively studied in the past. Human motion has been tracked by vision sensors [21], as well as based on the analysis of acceleration patterns [14], [8]. Furthermore, infrastructure-based localization has been studied, e.g. based on WLAN [6], and super-distributed RFID tag infrastructures [1], and also specifically in the context of emergency response [9], [18]. However, these methods are mainly designed from a single agent perspective, i.e. they do not exploit the potential advantage of data sharing.

Early work on SLAM was mainly based on the Extended Kalman Filter (EKF) [4]. Lu and Milios introduced a method for globally optimizing robot trajectories by building a constraint graph from LRF and odometry observations [16]. Whereas these methods typically rely on a high density of landmarks and require loops on single trajectories, RFID-SLAM is tailored for very sparse landmark distributions with reliable data association, and without requiring loops from single agents.

We conducted extensive experiments with a team of humans and robots within a semi-outdoor environment. Results from these experiments show that the introduced method allows to improve single trajectories based on the joint graph, even if they do not contain any loop.

The remainder of this paper is structured as follows. In Section II we introduce the utilized methods for robot and pedestrian pose tracking, respectively. In Section III the approach for centrally optimizing single agent trajectories is described. Finally, we provide results from robot experiments in Section IV and conclude in Section V.

## II. POSE TRACKING

We denote the two-dimensional pose of pedestrians and robots with the vector  $l = (x, y, \theta)^T$ . In order to represent uncertainties, the pose is modeled by a Gaussian distribution  $N(\mu_l, \Sigma_l)$ , where  $\mu_l$  is the mean and  $\Sigma_l$  a  $3 \times 3$  covariance matrix [17]. Both pedestrian and robot motion is measured by odometry consisting of the traveled distance  $d$  and angle  $\alpha$ , likewise modeled by a Gaussian distribution  $N(u, \Sigma_u)$ , where  $u = (d, \alpha)$  and  $\Sigma_u$  is a  $2 \times 2$  covariance matrix expressing odometry errors. The pose

at time  $t$  can be updated from input  $u_t$  as follows:

$$l_t = F(l_{t-1}, u_t) = \begin{pmatrix} x_{t-1} + \cos(\theta_{t-1})d_t \\ y_{t-1} + \sin(\theta_{t-1})d_t \\ \theta_{t-1} + \alpha_t \end{pmatrix}, \quad (1)$$

$$\Sigma_{l_t} = \nabla F_l \Sigma_{l_{t-1}} \nabla F_l^T + \nabla F_u \Sigma_u \nabla F_u^T, \quad (2)$$

$$\text{where } \Sigma_u = \begin{pmatrix} d\sigma_d^2 & 0 \\ 0 & \alpha\sigma_\alpha^2 \end{pmatrix} \quad (3)$$

and  $\nabla F_l$  and  $\nabla F_u$  are partial matrices of the Jacobian matrix  $\nabla F_{lu}$ . In the following we will describe the computation of input  $u_t$  from human and robot motion, respectively.

Dead reckoning information from human walking is acquired after a method that has been introduced by Ladetto et al. [14]<sup>1</sup>. Human walking generates a vertical acceleration with a maximum value if a foot is placed on the ground. By detecting these maxima in the vertical acceleration curve it is possible to detect and count the occurrence of footsteps. The direction estimate is coupled with an IMU (Inertial Measurement Unit), yielding the walking direction  $\theta$ . Finally, we utilize Equation 1 for dead reckoning, yielding the pose estimate  $(\hat{x}, \hat{y}, \hat{\theta})^T$  with covariance matrix  $\Sigma$ , from the successive integration of estimated distances  $\hat{d}$  and orientations  $\hat{\theta}$  with variance  $\sigma_{\hat{d}}^2$  and  $\sigma_{\hat{\theta}}^2$ , respectively. For our experiments we utilized the *MTi* IMU from *Xsens*, which combines a tri-axial accelerometer and a tri-axial gyroscope with a tri-axial magnetometer. Due to the simultaneous integration of gyro and compass data, the device provides a drift-free orientation vector that is stable towards minor perturbations caused by external magnetic sources. Based on an empirical evaluation, we modeled pose tracking uncertainty with  $\sigma_{\hat{d}}^2 = (0.05m/m)^2 d$ , and  $\sigma_{\hat{\theta}}^2 = (15^\circ)^2$ .

Dead reckoning on robots is usually error-prone due to wheel slippage, particularly within outdoor scenarios that are accompanied with different kinds of grounds. If the robot operates on slippery ground, as for example grass, or if it is likely that the robot gets stuck on obstacles, odometry errors are dependent on the particular situation. Therefore, we designed the *Zerg* robot (see Figure 1(b)) with an over-constrained odometry for the detection of slippage of the wheels by utilizing four shaft-encoders, one for each wheel. From these four encoders, we recorded data while the robot was driving on varying ground, and labeled the data sets with the classes  $C = (\textit{slippage}, \textit{normal})$ . This data was taken to learn a decision tree [20] with the inputs  $I = (\Delta v_{Left}, \Delta v_{Right}, \Delta v_{Front}, \Delta v_{Rear})$ , representing the velocity differences of the four wheels, respectively.

Given the detection of slippage, the traveled distance  $d$  is computed from the minimum wheel velocity, e.g.  $v_t = \min(v_{LeftFront}, v_{RightFront}, v_{LeftRear}, v_{RightRear})$ , and the robot’s pose is updated according to Equation 1 with  $\sigma_{d_{slip}}^2$ , within covariance matrix  $\Sigma_u$ , in order to increase uncertainty in translation. Note that the rotation

<sup>1</sup>We utilized an implementation from Michael Dippold [3]

update needs not to be modified since the traveled angle  $\alpha$  is measured by the IMU which is not affected by wheel slippage.

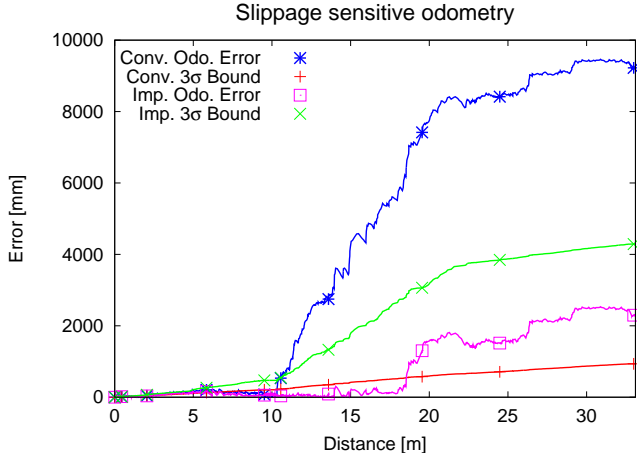


Fig. 2. Conventional odometry compared to slippage sensitive odometry during the event of slippage (between 10 and 20 meters): In contrast to conventional odometry, improved odometry reduces the position error and provides valid covariance bounds during slippage.

The values for  $\sigma_d^2$  and  $\sigma_{d_{slip}}^2$  have been determined experimentally within our laboratory. In this structured indoor environment it was possible to obtain ground truth by applying scan matching, a method that incrementally matches readings from a Laser Range Finder (LRF) for obtaining highly accurate pose displacements of the robot. During extensive runs that contained slippage events, the true traveled distance, determined by scan matching, and the distance estimated by the odometry has been recorded. The data set has been labeled by the slippage detection and then utilized for computing the Root Mean Square (RMS) error for determining the variances  $\sigma_d^2$  and  $\sigma_{d_{slip}}^2$ . We finally determined  $\sigma_d = 0.816 \frac{cm}{m}$  and  $\sigma_{d_{slip}} = 24.72 \frac{cm}{m}$ . As shown in Figure 2, the improved odometry reduces the error significantly while maintaining appropriate covariance bounds.

### III. RFID-SLAM

RFID-SLAM is a procedure for correcting odometry trajectories from multiple robots and humans by utilizing RFIDs for data association. For the sake of simplicity, we denote robots and humans as “field agents”, which communicate their observations to a central station. More specifically, the agents estimate distances between RFID locations by the pose tracking methods described in Section II, and communicate these estimates back to the station, which centrally combines and corrects all trajectories. Furthermore, it is assumed that RFID detections are within a range of  $< 1$  m, allowing to cover corridors and doorways, while providing sufficient positioning accuracy.

Each time an RFID has been observed, a message is generated that contains the ID of the previously visited

RFID  $i$  and currently visited RFID  $j$ , as well as an estimate of the local displacement between both RFIDs. The noisy measurement of the local displacement between two nodes is denoted by  $\hat{d}_{ij} = d_{ij} + \Delta d_{ij}$ . It is assumed that the error  $\Delta d_{ij}$  is normally distributed and thus can be modeled by a Gaussian distribution with zero mean and  $3 \times 3$  covariance matrix  $\Sigma_{ij}$ . The local displacement  $\hat{d}_{ij}$  is defined by the vector  $(\Delta \hat{x}_{ij}, \Delta \hat{y}_{ij}, \Delta \hat{\theta}_{ij})^T$ , whereas  $\Delta \hat{x}_{ij}$  and  $\Delta \hat{y}_{ij}$  denote the relative spacial displacement, and  $\Delta \hat{\theta}_{ij}$  the relative orientation change. Our goal is to compute a globally consistent map, i.e. to determine the true locations of the RFIDs from all observations communicated to the station.

We denote the true pose vectors of  $n+1$  RFID nodes by  $l_0, l_1, \dots, l_n$ , and the function calculating the true displacement  $(\Delta x_{ij}, \Delta y_{ij}, \Delta \theta_{ij})^T$  between a pair of nodes  $(l_i, l_j)$  is denoted as measurement function  $d_{ij}$ . The central station incrementally builds a global graph from all displacement estimates communicated by the field agents through utilizing the unique ID of RFIDs for data association. The constructed graph  $G = (V, E)$  consists of vertices  $V$  and edges  $E$ , where each vertex represents an RFID tag, and each edge  $(V_i, V_j) \in E$  represents an estimate  $\hat{d}_{ij}$  with covariance matrix  $\Sigma_{ij}$  between two RFID tags associated with vertices  $V_i$  and  $V_j$ , respectively. The subgraphs from all field agents are unified in the following way: On the one hand, if the same vertex has been observed twice, a loop has been detected in the graph. A detected loop is modeled by a *pseudo* edge between the same RFID node with distance  $\hat{d}_{ii}$  set to  $(0, 0, \Delta\theta)^T$ , whereas  $\Delta\theta$  denotes the angle difference between the two pose estimates of the RFID. Furthermore, under the assumption that RFIDs are detected at 95% probability if they are within maximal reading range  $d_M$ , we model the according covariance matrix by:

$$\Sigma_{ii} = \begin{pmatrix} 2^2 d_M^2 & 0 & 0 \\ 0 & 2^2 d_M^2 & 0 \\ 0 & 0 & \sigma_\theta^2 \end{pmatrix}, \quad (4)$$

whereas  $\sigma_\theta^2$  is the linearized variance of the angle, and  $2^2 d_M^2$  the variance of the normal distribution over the interval  $[-2d_M; 2d_M]$ . On the other hand, if two or more field agents observe the same edge, i.e. their trajectory overlaps between two or more neighboring RFIDs, both observations are merged by an Extended Kalman Filter (EKF).

Finally, the constructed graph, and thus the underlying map represented by RFID locations is globally corrected by minimizing the Mahalanobis distance [16]. Here, the goal is to find the true locations of the  $l_{ij}$  given the set of measurements  $\hat{d}_{ij}$  and covariance matrices  $\Sigma_{ij}$ . This can be achieved after the maximum likelihood concept by the following minimization:

$$l = \arg \min_l \sum_{i,j} \left( d_{ij} - \hat{d}_{ij} \right)^T \Sigma_{ij}^{-1} \left( d_{ij} - \hat{d}_{ij} \right), \quad (5)$$

where  $l$  denotes the concatenation of poses  $l_0, l_1, \dots, l_n$ . Since measurements are taken relatively, it is assumed without loss of generality that  $l_0 = 0$  and  $l_1, \dots, l_n$  are relative to  $l_0$ . Moreover, the graph is considered as fully connected, and if there does not exist a measurement between two nodes, the inverse covariance matrix  $\Sigma_{ij}^{-1}$  is set to zero. In order to solve the optimization problem analytically, Equation 5 can be transformed into matrix form [16]. Note that due to the angle  $\theta$  Equation 5 has to be linearized. The network of RFIDs can be optimized in  $O(n^3)$ , whereas  $n$  denotes the number of RFIDs.

We utilized two different RFID antennas for humans and robots. The antenna of the robot was mounted in parallel to the ground, allowing to detect RFIDs lying beneath the robot, whereas the antenna of the human was carried manually. We used Ario RFID chips from *Tagsys* with a size of  $1.4 \times 1.4$  cm, 2048 Bit RAM, and a response frequency of 13.56 MHz. For the reading and writing of these tags, we employed a Medio S002 reader, likewise from *Tagsys*, which is able to detect RFIDs within a range of approximately 30 cm with both antenna types. Hence, the covariance matrix in Equation 4 has been modeled with  $d_M = 30$  cm.

#### IV. EXPERIMENTAL RESULTS

We conducted extensive experiments with a team of humans and robots. During these experiments, ground truth data has been obtained with a *GPSlim236* GPS receiver from *Holux*, which is equipped with *Sirf Star III* technology. The receiver is able to receive Differential GPS (DGPS) data from the *EGNOS*<sup>2</sup> system, yielding a horizontal position accuracy  $< 2.2$  meters and vertical position accuracy  $< 5$  meters at 95 % of the time.

##### A. Pose tracking under heavy slippage

The slippage detection method has been extensively evaluated on the *Zerg* robot. During this experiment, the robot performed different maneuvers, such as moving straight, turning, and accelerating while driving first on normal and then on slippery ground. Afterwards, each situation has been manually labeled with one of the six classes *slip-straight*, *slip-turn*, *slip-accelerate*, *noslip-straight*, *noslip-turn*, and *noslip-accelerate*. Table I summarizes the results of the classification, where bold numbers indicate the correct classification, i.e. *true-positives*. As can be seen, the method is able to reliably detect slippage even while the robot is accelerating or performing turns.

##### B. Multi-Human Experiment

The multi-human experiment has been carried out on the campus of the University of Freiburg, which includes many accessible buildings entered by the test person. We measured that some of these buildings contain magnetic fields disturbing the angle estimate of the PDR method,

<sup>2</sup>EGNOS stands for European Geostationary Navigation Overlay Service.

Classification		Slip	No Slip
True situation			
Straight	No Slip	10 (0.5%)	<b>2051 (99.5%)</b>
	Slip	<b>2363 (90.1%)</b>	236 (8.9%)
Turn	No Slip	28 (0.9%)	<b>3226 (99.1%)</b>
	Slip	<b>2684 (96.4%)</b>	102 (3.6%)
(De-)Acceleration	No Slip	75 (14.9%)	<b>426 (85.1%)</b>
	Slip	<b>126 (98.5%)</b>	2 (1.5%)

TABLE I

CLASSIFICATION ACCURACY OF THE SLIPPAGE DETECTION.

as for example, metal stairs or metal doors. Figure 3 provides an overview of the area, which was generated by *GoogleEarth*. During this experiment, the test person traveled six trajectories with different starting and ending locations, while performing pose tracking with the PDR method previously described and while distributing and re-observing around 20 RFIDs (see Figure 3). In order

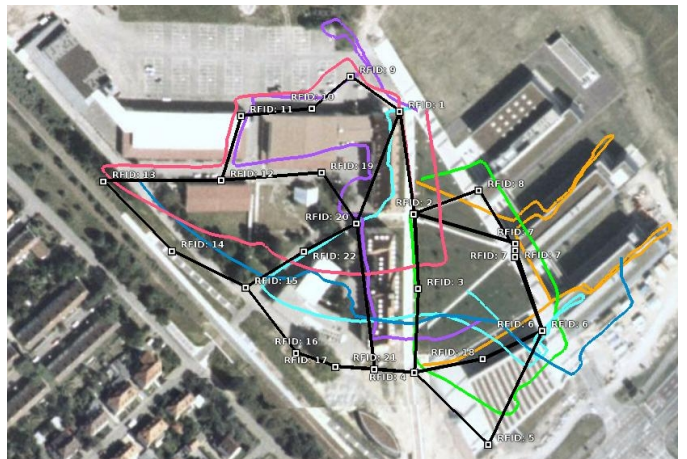


Fig. 3. Result from the multi-human experiment: Each line indicates the pose tracking of the trajectory of a single pedestrian. Black lines and squares show the corrected graph of RFIDs.

to visualize the PDR trajectories, we used the starting locations taken from the ground truth data and projected each PDR trajectory with respect to its starting location on the map. In Figure 3 each trajectory is shown with a different color. As can be seen, position accuracy decreases with increasing length of the traveled trajectory. Note that most of the trajectories do not include loops by themselves, making their single correction impossible.

All trajectories have been collected and merged into a joint graph for applying the centralized method described in Section III. The corrected edges between RFIDs are shown by the black lines in Figure 3, as well as the corrected locations of the RFIDs (small squares). Furthermore, we computed the average Cartesian error with respect to ground truth. Figure 4 depicts these errors according to each pedestrian. It shows the uncorrected trajectory, the single trajectory corrected on its own, and the trajectory corrected from the joined graph. As can be

seen, the correction based on the joined graph yields better results than the single corrections since the joining of single routes yields additional loops that support the correction.

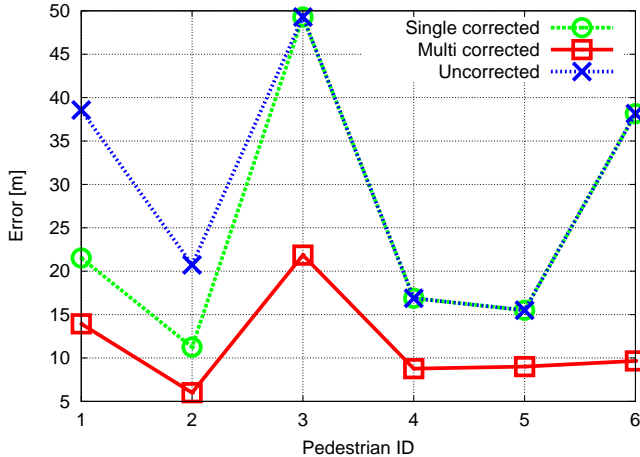


Fig. 4. Result from the multi-human experiment: the average Cartesian error of each pedestrian’s route.

### C. Human-Robot Experiment

In another experiment we jointly corrected the odometry trajectories from a human and robot exploring the same area while detecting RFIDs. During this experiment, pedestrian and robot performed pose tracking with the PDR method and slippage sensitive odometry described in Section II, while the robot navigated at an average velocity of 1.58 m/s. For an area of approximately  $90,000 m^2$ , only 10 RFIDs have been used, which is a comparably low amount of features considering the trajectory length of 2.5 km. Note that we already showed in former work that the RFID density does not significantly affect the correction of RFID-SLAM [11]. Table II depicts the average

	Cart. Err. [m]	XTE Err. [m]	ATE Err. [m]
Rob. Odo.	$147.10 \pm 36.85$	$139.59 \pm 35.99$	$46.11 \pm 20.69$
Ped. Odo.	$56.63 \pm 24.38$	$44.22 \pm 24.52$	$32.31 \pm 15.82$
Ped. Corr.	$14.27 \pm 12.7$	$8.40 \pm 11.67$	$10.68 \pm 10.84$
Rob. Corr.	$9.37 \pm 9.90$	$5.57 \pm 9.55$	$6.52 \pm 9.23$
Both Corr..	$5.64 \pm 4.77$	$2.50 \pm 4.23$	$4.33 \pm 4.50$

TABLE II

AVG. POS. ERRORS OF ODOMETRY, SINGLE, AND JOINT CORRECTION.

Cartesian error, the average cross-track error (XTE), and average along-track error (ATE) of the original robot odometry (Rob. Odo.), the original pedestrian odometry (Ped. Odo.), their single corrected trajectories (Ped. Corr, Rob Corr.), and the jointly corrected trajectory (Both Corr.). As can be seen, the simultaneous correction of both trajectories improved the accuracy significantly. Figure 5 (a) shows the both odometry trajectories compared to ground truth (blue line), and Figure 5 (b) shows the

corrected RFID graph (green line). Note that the small squares indicate RFID observations. Figure 6 depicts the covariance bounds of the robot trajectory before and after the global correction, showing the successful reduction of pose uncertainties by the optimization. Note that for the sake of readability, Figure 6 only shows the first loop of the performed trajectory.



(a)



(b)

Fig. 5. Result from correcting trajectories from robot odometry (orange line) and pedestrian odometry (red line) jointly: The corrected RFID graph (green line) lies close to ground truth (blue line). Small squares indicate RFID observations.

## V. CONCLUSIONS AND FUTURE WORKS

We introduced a novel method for jointly correcting trajectories of human and robot teams by utilizing the advantage of RFID technology for data association. Thereby, pose tracking has been carried out by sensors that are applicable within harsh environments. In contrast to vision

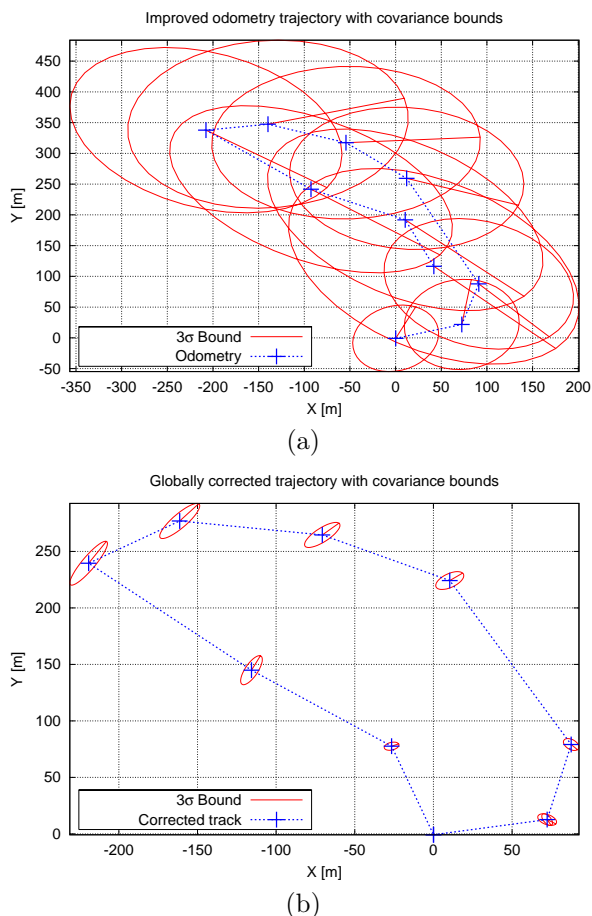


Fig. 6. Covariance bounds from applying RFID-SLAM with slippage sensitive odometry: (a) before and (b) after the global correction.

and laser scan matching based approaches, robot tracking was simply based on slippage sensitive wheel odometry and IMU data, and human tracking on a light-weight IMU sensor. Nevertheless, both systems produced acceptable estimates that have been successively corrected.

The introduced method allows to apply SLAM without requiring pedestrians and robots to perform loops while executing their primary task. Due to the joining of routes via RFID connection points, loops automatically emerge. This is a necessary requirement if applying SLAM within USAR situations. In such situations, emergency responders have time-critical goals that have to be accomplished within a short amount of time, hence intentionally try to avoid to visit places repeatedly. The result shows clearly that sharing information between single agents, i.e. humans and robots, allows to correct their individual paths globally.

In future work, we will investigate the approach within purely indoor environments and focus on correcting three-dimensional trajectories, e.g. within multi-storey buildings. Furthermore, we will evaluate RFID technology operating in the UHF frequency domain, allowing reading and writing within distances of meters, and to extend our

approach accordingly.

## REFERENCES

- [1] J. Bohn and F. Mattern. Super-distributed RFID tag infrastructures. In *Proceedings of the 2nd European Symposium on Ambient Intelligence (EUSAI 2004)*, number 3295, pages 1–12, The Netherlands, November 2004. Springer Verlag.
- [2] J. Borenstein and Feng. L. Measurement and correction of systematic odometry errors in mobile robots. *IEEE Journal of Robotics and Automation*, 12(6):869–880, 1996.
- [3] M. Dippold. Personal dead reckoning with accelerometers. In *IFAWC*, 2006.
- [4] M.W.M.G. Dissanayake, P. Newman, S. Clark, H.F. Durrant-Whyte, and M. Csorba. A solution to the simultaneous localization and map building (SLAM) problem. *IEEE Transactions on Robotics and Automation*, 17(3):229–241, 2001.
- [5] R. Fachberger, G. Bruckner, L. Reindl, and R. Hauser. Tagging of metallic objects in harsh environments. In *Sensoren und Messsysteme - 13. ITG-/GMA Fachtagung*, University of Freiburg, 2006.
- [6] A. Kealy G. Retscher. Ubiquitous positioning technologies for modern intelligent navigation systems. *The Journal of Navigation*, 59:91–103, 2006.
- [7] M.S. Grewal, L. R. Weill, and A. P. Andrews. *Global Positioning Systems, Inertial Navigation, and Integration*. John Wiley & Sons, 2001.
- [8] D. C. T. Judd. A personal dead reckoning module. In *Proc. of the Inst. of Navigation's GPS Conf.*, pages 169 – 170, 1997.
- [9] G. Kantor, S. Singh, R. Peterson, D. Rus, A. Das, V. Kumar, G. Pereira, and J. Spletzer. Distributed search and rescue with robot and sensor team. In *Proc. of the Fourth Int. Conf. on Field and Service Robotics*, pages 327–332. Sage Publications, 2003.
- [10] A. Kleiner, N. Behrens, and H. Kenn. Wearable computing meets multiagent systems: A real-world interface for the RoboCupRescue simulation platform. In N. Jennings, M. Tambe, T. Ishida, and S. Ramchurn, editors, *First International Workshop on Agent Technology for Disaster Management at AAMAS06*, Hakodate, Japan, 2006.
- [11] A. Kleiner and C. Dornhege. Real-time localization and elevation mapping within urban search and rescue scenarios. *Journal of Field Robotics*, 2007. Accepted for publication.
- [12] A. Kleiner, J. Prediger, and B. Nebel. RFID technology-based exploration and SLAM for search and rescue. In *Proc. of the IEEE/RSJ Int. Conf. on Intelligent Robots and Systems (IROS)*, Beijing, China, 2006.
- [13] Q. Ladetto and B. Merminod. In step with INS: Navigation for the blind, tracking emergency crews. *GPSWorld*, pages 30–38, 2002.
- [14] Q. Ladetto, B. Merminod, P. Terrirt, and Y. Schutz. On foot navigation: When GPS alone is not enough. *Journal of Navigation*, 53(02):279–285, Mai 2000.
- [15] W. Lechner, S. Baumann, and K. Legat. Pedestrian navigation - bases for the next mass market in mobile positioning. In *Proceedings of Locellus 2001*, pages 79–90, Munich, Germany, 2001.
- [16] F. Lu and E. Milios. Globally consistent range scan alignment for environment mapping. *Auton. Robots*, 4:333–349, 1997.
- [17] P. S. Maybeck. *Stochastic models, estimation, and control*, volume 141 of *Mathematics in Science and Engineering*. Academic Press, 1979.
- [18] L.E. Miller, P. F. Wilson, N. P. Bryner, Francis, J. R. Guerrieri, D. W. Stroup, and L. Klein-Berndt. RFID-assisted indoor localization and communication for first responders. In *Proc. of the Int. Symposium on Advanced Radio Technologies*, 2006.
- [19] L. Ojeda and J. Borenstein. Methods for the reduction of odometry errors in over-constrained mobile robots. *Autonomous Robots*, 16:273–286, 2004.
- [20] J. R. Quinlan. Induction of decision trees. *Machine Learning*, 1(1):81–106, 2003.
- [21] Z. Zhu, T. Oskiper, O. Naroditsky, S. Samarasekera, H. S. Sawhney, and R. Kumar. An improved stereo-based visual odometry system. USA, August 2006.